Cell Stem Cell
Article

N-Cadherin Expression Level Distinguishes Reserved versus Primed States of Hematopoietic Stem Cells

Jeffrey S. Haug,[1,4] Xi C. He,[1,4] Justin C. Grindley,[1] Joshua P. Wunderlich,[1] Karin Gaudenz,[1] Jason T. Ross,[1,3] Ariel Paulson,[1] Kathryn P. Wagner,[1] Yucai Xie,[1] Ruihong Zhu,[1] Tong Yin,[1] John M. Perry,[1] Mark J. Hembree,[1] Erin P. Redenbaugh,[1] Glenn L. Radice,[2] Christopher Seidel,[1] and Linheng Li[1,3,*]

[1]Stowers Institute for Medical Research, 1000 East 50th Street, Kansas City, MO 64110, USA

[2]Department of Obstetrics and Gynecology, Center for Research on Reproduction and Women's Health, University of Pennsylvania School of Medicine, Philadelphia, PA 19104, USA

[3]Department of Pathology and Laboratory Medicine, Kansas University Medical Center, Kansas City, KS 66160, USA

[4]These authors contributed equally to this work.

*Correspondence: lil@stowers-institute.org

DOI 10.1016/j.stem.2008.01.017

SUMMARY

Osteoblasts expressing the homophilic adhesion molecule N-cadherin form a hematopoietic stem cell (HSC) niche. Therefore, we examined how N-cadherin expression in HSCs relates to their function. We found that bone marrow (BM) cells highly expressing N-cadherin (N-cadherin^{hi}) are not stem cells, being largely devoid of a Lineage^{-}Sca1^{+}cKit^{+} population and unable to reconstitute hematopoietic lineages in irradiated recipient mice. Instead, long-term HSCs form distinct populations expressing N-cadherin at intermediate (N-cadherin^{int}) or low (N-cadherin^{lo}) levels. The minority N-cadherin^{lo} population can robustly reconstitute the hematopoietic system, express genes that may prime them to mobilize, and predominate among HSCs mobilized from BM to spleen. The larger N-cadherin^{int} population performs poorly in reconstitution assays when freshly isolated but improves in response to overnight in vitro culture. Their expression profile and lower cell-cycle entry rate suggest N-cadherin^{int} cells are being held in reserve. Thus, differential N-cadherin expression reflects functional distinctions between two HSC subpopulations.

INTRODUCTION

It is well accepted that stem cell niches play critical roles in the regulation of hematopoietic stem cell (HSC) behavior (Schofield, 1978). In BM, HSCs reside in "osteoblastic" (Arai et al., 2004; Calvi et al., 2003; Zhang et al., 2003) and "vascular" niches (Kiel et al., 2005), which may have complementary functions (Kopp et al., 2005; Yin and Li, 2006).

In the osteoblastic niche, HSCs associate with a subset of osteoblasts lining the endosteal surface that express N-cadherin (Cdh2, a calcium-dependent adhesion molecule) (Arai et al., 2004; Zhang et al., 2003). Accumulated evidence suggests that cadherins are not only required for stem cell anchoring to the niche (Song and Xie, 2002) but also influence the cycling state of HSCs (Wilson et al., 2004). The cycling state of HSCs is linked to their potential, as measured by reconstitution assay. Notably, quiescent subpopulations of HSCs are enriched with long-term (LT) HSCs capable of sustaining hematopoiesis for many months, whereas cycling HSC subpopulations are enriched with short-term (ST) HSCs unable to sustain reconstitution beyond a few weeks (Fleming et al., 1993).

It is believed the most primitive quiescent HSCs anchored in the niches have the most efficient reconstitution (Arai et al., 2004), but it is not yet known whether there is any direct relationship between expression of niche-interaction molecules such as N-cadherin and the properties of HSCs. We hypothesized that N-cadherin, present at the interface between HSCs and the osteoblastic niche in both mice and humans (Arai et al., 2004; Muguruma et al., 2006; Zhang et al., 2003), would identify quiescent HSCs and thus expected BM cells or HSCs expressing high levels of N-cadherin to have robust reconstitution activity. We found, however, that BM cells with the highest levels of N-cadherin expression were not HSCs. Instead, expression of N-cadherin at intermediate (N-cadherin^{int}) or low (N-cadherin^{lo}) levels divided HSCs into two populations with numerous molecular and functional distinctions. Our data suggest N-cadherin^{lo} HSCs fulfill ongoing hematopoiesis, whereas N-cadherin^{int} HSCs are held in reserve to support LT maintenance of the hematopoietic system.

RESULTS

LT-HSCs Predominantly Express Low-to-Intermediate Levels of N-Cadherin

N-cadherin may mediate niche interaction, so we tested whether N-cadherin^{+} HSCs could reconstitute the hematopoietic system. Using a polyclonal anti-N-cadherin antibody, we previously found that 10% of Lin^{-}Sca1^{+}cKit^{+} (LSK) stem and progenitor cells express N-cadherin (Zhang et al., 2003). In this study, we instead used a rat-anti-mouse N-cadherin monoclonal antibody (mAb) that exhibited superior specificity for mouse N-cadherin (see Figure S1 available online). In fluorescence-activated cell

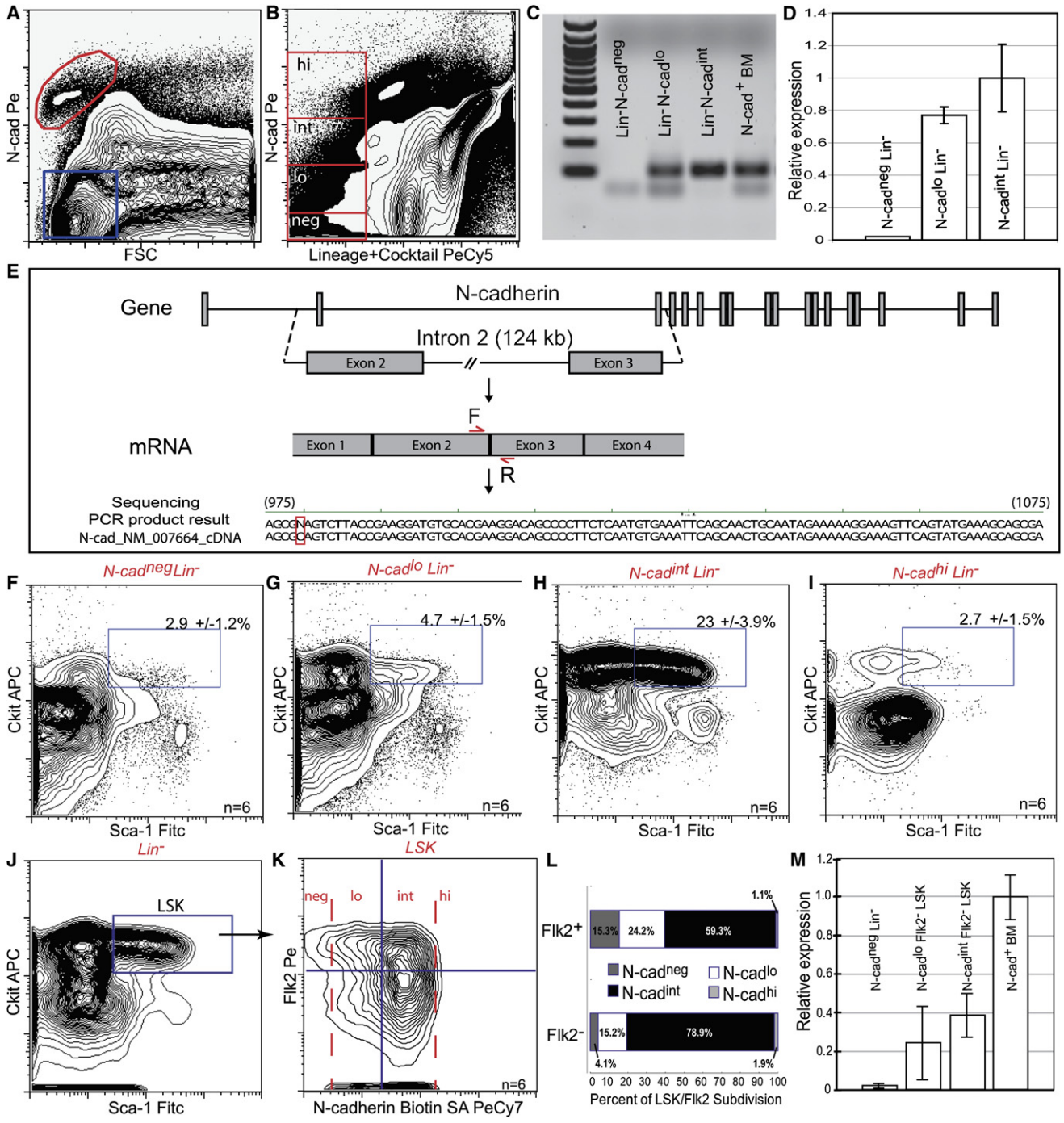

Figure 1. Examination of N-Cadherin Expression in Bone Marrow and HSCs

(A) Analysis of N-cadherin^{+} cells in BM using flow cytometry. Colored outlines indicate N-cadherin positive (red) and low/negative (blue) BM populations selected for transplant.

(B) Levels of N-cadherin in Lin^{-} cells assessed by flow cytometry. Lineage-negative (Lin^{-}) cells were further separated into subpopulations according to N-cadherin expression: negative, low, intermediate, and high (red boxes). The upper threshold of FMO controls provides the lower limit of signal in the N-cadherin^{int} population. The term N-cadherin^{lo} applies to the population just below this boundary because these cells are mRNA-positive and brighter on the N-cadherin axis in FACS than the dimmest, mRNA-negative ones.

(C and D) Real-time RT-PCR detection of N-cadherin mRNA. Shown are representative products (C) and a relative expression obtained from triplicate reactions (D). BM was used as positive control. Error bar is 1 SD.

(E) N-cadherin RT-PCR strategy and specificity. RT-PCR primers span exon2/3 junction interrupted by 124 kb intron in genomic DNA. Product sequenced with RT-PCR primers has >99% identity with N-cadherin reference sequence (NM_007664).

(F–I) LSK content of Lin^{-} populations with varying N-cadherin levels.

sorting (FACS), this mAb detected a distinct population representing 0.78% ± 0.6% (n = 12) of the total BM (Figure 1A). Transplanting 5000 cells, we found that N-cadherin-expressing BM failed to reconstitute hematopoietic lineages in recipient mice, yet BM with only limited N-cadherin expression reconstituted in one of five cases (Table S1). Surprised by this result, we explored N-cadherin expression further, separating BM into mature (lineage-positive, Lin^+) hematopoietic cells (Christensen and Weissman, 2001) and a Lin^- population known to be enriched with stem and progenitor cells. In multiparameter FACS, it can be challenging to distinguish dim fluorescent cells from the truly negative. To address this, we employed fluorescence minus one (FMO) staining controls, combinatorial panels that omit each fluorescent reagent or replace it with an isotype control (Roederer, 2001), and we combined FACS with RT-PCR. Within the Lin^- cell population, four different subpopulations were observed based on the expression level of N-cadherin: negative (N-$cadherin^-$), N-$cadherin^{lo}$, N-$cadherin^{int}$, and N-$cadherin^{hi}$ (Figure 1B). The N-$cadherin^{hi}$ population was predominantly Lin^+ (Figure 1B), explaining its failure to reconstitute. Real-time RT-PCR confirmed N-cadherin mRNA was present in Lin^-N-$cadherin^+$ cells, including Lin^-N-$cadherin^{lo}$ and Lin^-N-$cadherin^{int}$ cells, but not in the Lin^-N-$cadherin^-$ cells (Figures 1C and 1D). Amplicon specificity was confirmed by DNA sequence analysis (Figure 1E). These four subpopulations of Lin^- cells exhibited distinct Sca-1/cKit expression profiles (Figures 1F–1I), with N-$cadherin^{int}$ cells being most enriched with LSK stem and progenitors (23%). For these and all subsequent figures, red italic type indicates gating strategies of the displayed cells, and horizontal and vertical region markers are set using FMO controls.

Next, we analyzed the LSK cells by using N-cadherin and Flk2, which has been shown to separate LT ($Flk2^-$) and ST ($Flk2^+$) HSCs (Christensen and Weissman, 2001) (Figures 1J and 1K). We found the LSKs were mainly composed of N-$cadherin^{lo}$ and N-$cadherin^{int}$ cells. LT-HSCs ($Flk2^-$LSKs) were almost exclusively N-$cadherin^{int}$ or N-$cadherin^{lo}$; N-$cadherin^-$ cells were mainly $Flk2^+$, while N-$cadherin^{hi}$ cells were rarely detected (Figures 1K and 1L). Real-time RT-PCR confirmed the expression of N-cadherin mRNA in both N-$cadherin^{lo}$ and N-$cadherin^{int}Flk2^-$LSK cells compared to Lin^-N-$cadherin^-$ cells (Figure 1M; Figure S2). Since our focus was LT-HSCs, FACS gating hereafter was designed to separate N-$cadherin^{int}$ from N-$cadherin^{lo}$.

To locate N-$cadherin^+$ HSCs on BM sections, we used a mouse line (*N-cadherin-LacZ*) with a LacZ reporter gene trapped in at the N-cadherin locus (Luo et al., 2005) and CD201, a marker shown to explicitly identify HSCs (Balazs et al., 2006) (Supplemental Experimental Procedures). The majority of the BM cells were LacZ negative. Morphologically, the N-cadherin-$LacZ^{hi}$ BM cells appeared to be mature cells with irregular nuclei and a high cytoplasm to nucleus ratio (red arrows in Figures S3A and S3B). This further explained why N-$cadherin^{hi}$ BM lacked reconstitution activity. Consistent with previous findings that HSCs attach to spindle-shaped N-$cadherin^+$ osteoblasts (Zhang et al., 2003), we detected moderate N-cadherin-LacZ expression in $CD201^+$ cells adjacent to osteoblasts that were strongly positive for LacZ (Figures S3C–S3E).

N-$Cadherin^{lo}Flk2^-$LSK Cells Robustly Repopulate Hematopoietic Lineages in Recipient Mice

We performed competitive repopulation assays to determine if N-$cadherin^+$LSK cells contain functional HSCs. Consistent with a previous report (Christensen and Weissman, 2001), the $Flk2^+$LSK cells rarely reconstituted the hematopoietic lineages long-term (data not shown). We transplanted 25 N-$cadherin^{lo}$ or 25 N-$cadherin^{int}$ $Flk2^-$LSK cells ($CD45.2^+$) into lethally irradiated recipient mice ($CD45.1^+$). N-$cadherin^{lo}$ donor cells gave higher engraftment of multiple hematopoietic lineages (four of five mice exhibited engraftment; average 53%) than N-$cadherin^{int}$ (two of five engrafting; average 1.4%), a result typical of several replicate experiments (Figure 2A, Table S1). As $Slamf1^+$ (CD150) HSCs are reported to be enriched with LT-HSCs (Kiel et al., 2005), we also assayed $CD150^+$ $Flk2^-$LSKs. $CD150^+$ LSKs were enriched in $Flk2^-$LSK and represented 12.5%–25% of the $Flk2^-$LSK population (Figure 2B). Average engraftment of $CD150^+Flk2^-$LSKs (3.2%) was low compared to N-$cadherin^{lo}Flk2^-$LSKs (53%) but better than N-$cadherin^{int}Flk2^-$LSKs (1.4%) (Figure 2C) and contrasts with the strongly reconstituting SLAM code HSCs previously isolated as $CD150^+$ $CD48^-CD41^-$ (Kiel et al., 2005). This difference likely stems from use of the negative markers CD48 and CD41. Specifically, $CD150^+CD48^-CD41^-$ cells (Figure 2D) were predominately (67.5%) N-$cadherin^{lo}Flk2^-$ cells (Figure 2E), whereas just 14% of $CD150^+Flk2^-$LSK were N-$cadherin^{lo}$ (Figure 2F).

Overnight In Vitro Culture Improves the Reconstitution Activity of N-$Cadherin^{int}Flk2^-$LSK

We next asked whether N-$cadherin^{int}$ and N-$cadherin^{lo}$ $Flk2^-$LSK retained their distinct N-cadherin expression and reconstitution ability upon overnight culture in serum-free STIF media (Zhang et al., 2006). N-cadherin expression levels prior to culture were compared to those observed in the same cells restained with the mAb postculture. To control for differences in HSC staining/handling, we restained cells held at 4°C in STIF but not cultured. Culturing the N-$cadherin^{lo}$ population generated a sizable population of non-LSK cells (Figures 2G–2I). In contrast, culturing shifted a majority of N-$cadherin^{int}$ cells to N-$cadherin^{lo}$ (Figures 2J and 2L) while retaining a large portion of the cells as LSK (Figure 2K). N-$cadherin^{int}$ cells held at 4°C resembled the input population. To assess the functional impact of culture, we transplanted 25 or 100 freshly isolated cells or overnight cultured cells derived from the same number of input cells (we used 100 N-$cadherin^{int}$ $Flk2^-$LSKs, since 25 fresh cells had given minimal reconstitution). The culture step increased the engraftment rate of 100 N-$cadherin^{int}$ $Flk2^-$LSK to an average of 14.2% (Figure 2M), whereas it reduced the average engraftment of 25 N-$cadherin^{lo}$ $Flk2^-$LSKs (compare Figures 2C and 2M).

(J–M) Analyses of LSK cells with Flk2 and N-cadherin markers using flow cytometry. (J) Isolation of LSK population. (K) Subdivision of LSK by Flk2 and N-cadherin. Divisions of N-cadherin expression (neg, lo, int, and hi) applied signal thresholds in the same relative positions as those used for the Lin^- population (B). (L) Proportions of N-$cadherin^-$, N-$cadherin^{lo}$, and N-$cadherin^{int}$ and N-$cadherin^{hi}$ in $Flk2^+$ and $Flk2^-$LSK cells. (M) Determination of N-cadherin mRNA levels in LT-HSCs using real-time RT-PCR. Error bar is 1 SD; number of cells, 400.

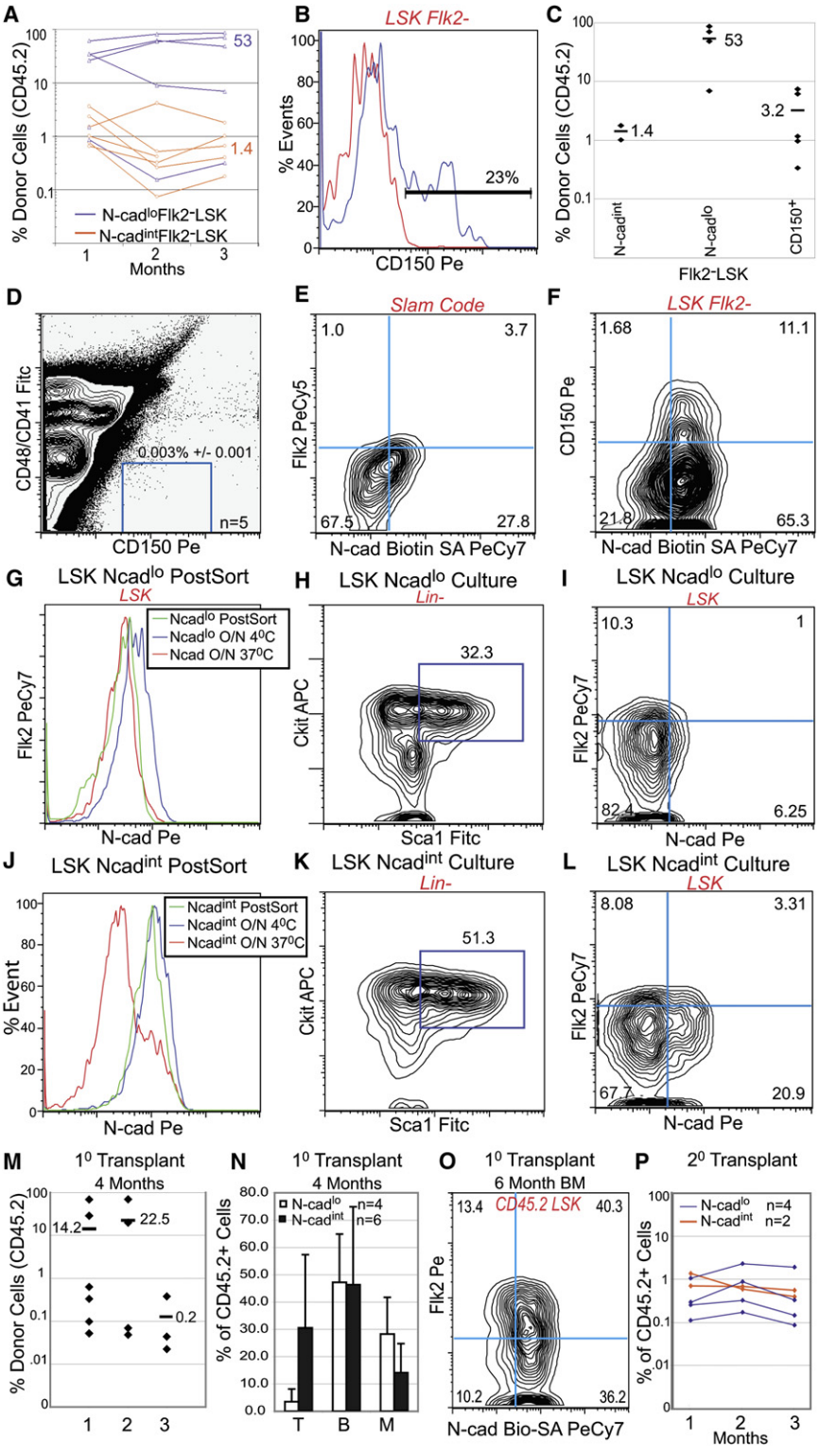

Figure 2. Functional Comparison of N-Cadherin^{lo} and N-Cadherin^{int} Flk2$^-$LSK Cells with CD150$^+$Flk2$^-$LSK Cells

(A) Reconstitution activity of 25 N-cadherin^{lo} (blue) and N-cadherin^{int} (orange) Flk2$^-$LSK cells. At 1, 2, and 3 months, engraftment was measured by flow cytometry analysis of donor (CD45.2) cells present in recipient PB. Values indicate average engraftment at 3 months.

(B) Analysis of CD150 expression in Flk2$^-$LSKs. Representative histogram shows CD150 signal (blue) and FMO isotype control (red). Bar indicates CD150$^+$ population.

(C) Comparison of the reconstitution activity of 25 CD150$^+$, N-cadherin^{lo}, and N-cadherin^{int} Flk2$^-$LSKs. Graph shows the individual (◆) and average (—) percentage of PB CD45.2 cells present in engrafted recipients at 3 months posttransplant.

(D) Representative analysis of BM using the standard SLAM code method. Proportion of CD150$^+$CD48$^-$CD41$^-$ cells shown is average of five experiments.

(E) Analysis of BM SLAM code cells, gated as in (D), for N-cadherin and Flk2.

(F) N-cadherin and CD150 expression in Flk2$^-$LSKs.

(G–L) Impact of overnight incubation in STIF medium on N-cadherin^{lo} Flk2$^-$LSKs (N-cad^{lo}) (G–I) and N-cadherin^{int} Flk2$^-$LSKs (N-cad^{int}) (J–L). (G and J) Comparison of N-cadherin expression before (green) and after (red) 16 hr culture in STIF medium at 37°C, as well as cells held at 4°C (blue). (H and K) Assessment of LSK content after overnight culture. Proportion of LSKs is indicated above the gate. (I and L) N-cadherin and Flk2 expression in LSKs isolated from overnight cultures of cultured N-cad^{lo} and N-cad^{int} cells.

(M) Reconstitution activity of 100 STIF cultured N-cadherin^{int} Flk2$^-$LSKs (#1), 25 STIF cultured N-cadherin^{lo} Flk2$^-$LSKs (#2), and 100 freshly isolated N-cadherin^{int} Flk2-LSK cells (#3) in primary transplant recipients analyzed at 4 months. Percentages of donor (CD45.2) cells in PB are shown for individual engrafted recipients (◆) and as averages (—).

(N) Following culture, N-cadherin^{int} and N-cadherin^{lo} Flk2-LSKs give multilineage engraftment 4 months after primary transplant. BM of the engrafted recipients was analyzed for donor-derived (CD45.2) B220 (B cells, "B"), CD3 (T cells, "T"), and mac1$^+$/Gr1$^+$ (myeloid cells, "M"). Error bar is 1 SD.

(O) N-cadherin and Flk2 expression in donor-derived BM LSKs 6 months following primary transplantation of cultured N-cadherin^{int} Flk2-LSKs.

(P) Reconstitution activity of 100 donor-derived BM LSKs from primary recipients of cultured N-cadherin^{lo} (blue) and cultured N-cadherin^{int} (orange) Flk2$^-$LSK cells. Donor (CD45.2) contribution to secondary recipient PB was assessed at 1, 2, and 3 months. All engrafted recipients (2 of 7 for N-cadherin^{int}; 4 of 10 for N-cadherin^{lo}) are shown.

Cultured N-cadherin^{int} Flk2$^-$LSKs provided effective reconstitution of all lineages examined (T, B, and myeloid) (Figure 2N). They also gave rise to LSKs whose profile of Flk2 and N-cadherin expression resembled that of normal nontransplanted mice (compare Figures 2O and 1K). Six months after the initial transplant, we performed secondary transplants from well-engrafted primary recipients. We found that, whether originating from cultured N-cadherin^{int} or cultured N-cadherin^{lo} Flk2$^-$LSKs, 100

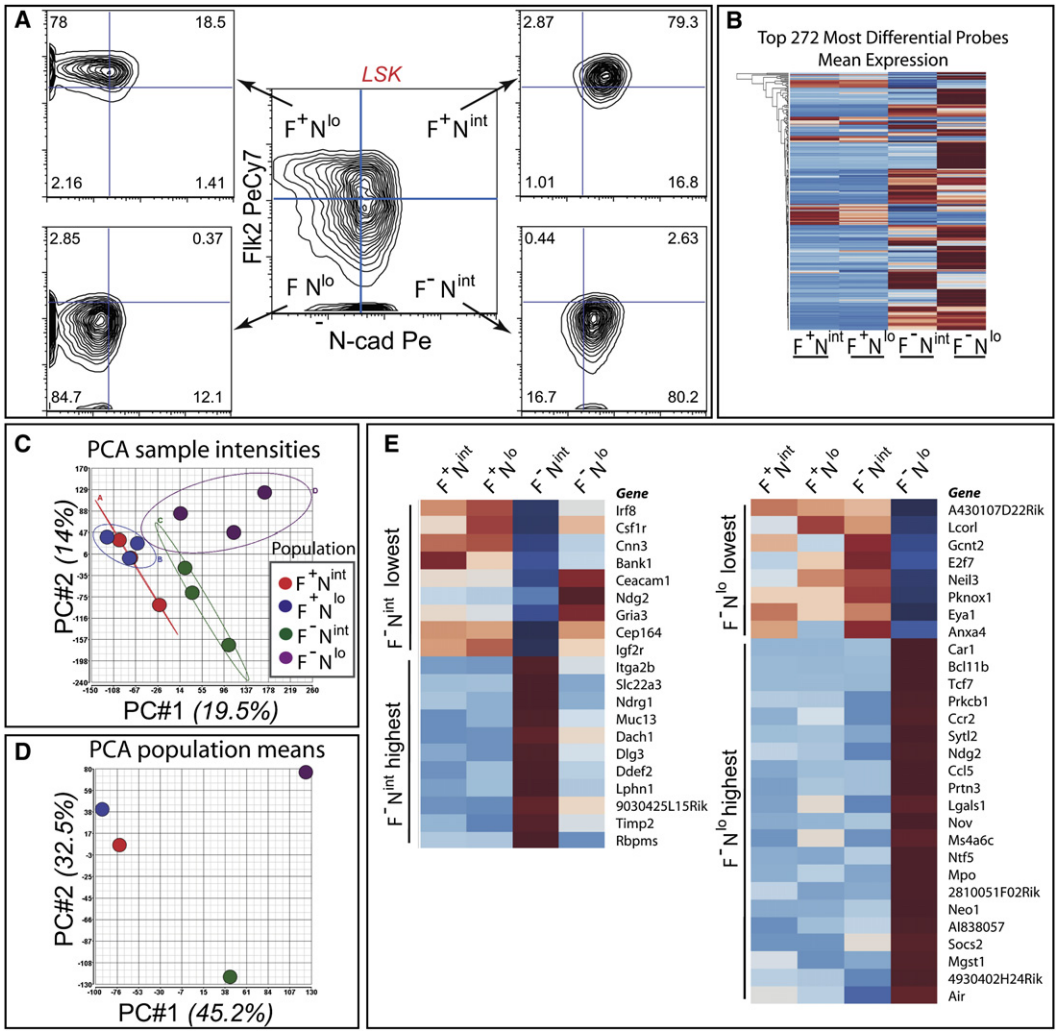

Figure 3. Gene Expression Profiles Distinguish N-Cadherin^{int} and N-Cadherin^{lo} Flk2^{-}LSKs

(A) Separation of LSKs into four populations for microarray analysis according to N-cadherin (N) and Flk2 (F) expression (F^+N^{lo}, F^+N^{int}, F^-N^{lo}, F^-N^{int}). Gating strategy (center) is flanked by representative postsorts showing the purity of the four populations after the first of two serial FACS sorts.

(B) Heat map representation of variation across the four populations (red, high expression; blue, low expression) of the 272 most differential array probes clustered by similar expression profiles.

(C and D) Principal component (PC) analysis performed on raw array intensities for all samples (C) or on background-corrected, normalized population means (D). Plots show average expression data in the plane defined by the first two PCs of the data set (PC#1, PC#2). Proportions of total data variance attributed to each PC are indicated in parentheses. Ellipses in (C), standard errors for the population means, have minimal or no overlap when an axis effectively separates the populations.

(E) Heat maps illustrating the expression profiles of genes both differentially expressed between F^-N^{int} and F^-N^{lo} (>1.75-fold) and with highest or lowest expression occurring in population F^-N^{int} (left) or F^-N^{lo} (right).

donor-derived LSKs provided effective reconstitution for secondary recipients 3 months after transplantation (Figure 2P) and contributed to T, B, and myeloid lineages (data not shown). Thus, N-cadherin^{int}Flk2^{-}LSKs do have the capacity to provide LT multilineage reconstitution if transplanted postculture rather than as freshly isolated cells.

N-Cadherin Level Separates Flk2^{-}LSKs into Molecularly Distinct Populations

To build gene-expression profiles of stem and progenitor cells with different N-cadherin levels, we sorted LSKs into four populations according to surface Flk2 and N-cadherin expression (Figure 3A), resorted to increase purity, and performed triplicate microarray studies. Sorting directly into Trizol for RNA preparation precluded determination of final purities, but the first FACS step gave purities around 80%, and equivalent double-sorted populations were around 95% pure. Most genes varied little among these populations. Analysis of probes with the most differential signals (see the Supplemental Experimental Procedures) revealed that the Flk2^{+} populations (F^+N^{lo} and F^+N^{int}) commonly gave similar signal levels but were distinct from the two Flk2^{-} populations (F^-N^{lo} and F^-N^{int}), which in turn frequently differed from each other (Figure 3B). Thus, N-cadherin levels separated Flk2^{-} LT-HSCs into distinct populations but had

limited impact on the expression profile of Flk2$^+$ ST-HSCs and progenitors. Principal component analysis (PCA) (Figure 3C), which identifies and orders sources of variation within large data sets (Raychaudhuri et al., 2000) (see the Supplemental Experimental Procedures), demonstrated that Flk2 status was the most significant determinant of variation among the four populations. Whether PCA was performed on all samples (Figure 3C) or on population means (Figure 3D), the first principal component (PC1, responsible for the greatest variation in the data set) separated populations F$^+$N^{lo} and F$^+$N^{int} from populations F$^-$N^{lo} and F$^-$N^{int}. Moreover, Flk2 mRNA expression was very strongly correlated (Pearson correlation coefficient r = −0.97931) with the population mean PC1 axis.

PC2, the next largest source of variation in the data set, separated populations F$^-$N^{lo} and F$^-$N^{int}, but not F$^+$N^{lo} and F$^+$N^{int}. F$^-$N^{lo} and F$^-$N^{int} were defined on the basis of surface N-cadherin protein, yet N-cadherin mRNA levels only weakly correlated with the population mean PC2 (r = −0.60), perhaps implying additional posttranscriptional control. Real-time RT-PCR similarly showed that N-cadherin^{lo} and N-cadherin^{int} populations differ only modestly in N-cadherin mRNA levels. Gene ontology analysis for genes highly correlated with PC2 ($|r| > 0.95$) indicated that the cell populations separated by this axis likely differed in metabolic status, signaling, and cell-cycle control (Table S2). Genes positively correlated with PC2 (more highly expressed in F$^-$N^{lo} than in F$^-$N^{int}) were involved in protein biosynthesis and nucleotide metabolism, suggesting that N-cadherin^{lo} HSCs may be more active than their N-cadherin^{int} counterparts. Conversely, the negatively correlated gene set (expressed more highly in F$^-$N^{int}) was overrepresented in genes encoding insulin signaling pathway components, regulators of signal transduction, and cell-cycle proteins.

N-Cadherin^{int} and N-Cadherin^{lo} Stem Cells Differ in Expression of Key HSC Regulators

To help identify the basis of their distinct reconstitution abilities, we identified genes with a >1.75-fold difference in expression between populations F$^-$N^{int} and F$^-$N^{lo}, focusing on those in which F$^-$N^{int} or F$^-$N^{lo} expression was the highest or lowest of the four populations examined (see the Supplemental Experimental Procedures). This generated 48 genes in four sets (F$^-$N^{int} lowest, F$^-$N^{int} highest, F$^-$N^{lo} lowest, and F$^-$N^{lo} highest) (Figure 3E; Table S3).

Genes with highest expression in F$^-$N^{lo}, the population with the greatest reconstitution ability, included chemokine (C-C motif) receptor 2 (Ccr2), chemokine (C-C motif) ligand 5 (Ccl5), and neurotrophin 5(Ntf5), all of which are involved in locomotor activity or chemotaxis (Moser et al., 2004; Tucker et al., 2001). In contrast to the high Ccr2 mRNA expression observed in F$^-$N^{lo}, we found that the poorly reconstituting F$^-$N^{int} population showed particularly low levels of colony-stimulating factor 1 receptor (Csf1r) and insulin-like growth factor 2 receptor (Igf2r) mRNAs, suggesting differential responsiveness to signaling molecules. Igf2r may be regulated by different mechanisms in F$^-$N^{lo} and F$^-$N^{int}, since F$^-$N^{lo} had high levels of Air, the Igf2r antisense transcript (Sleutels et al., 2002). Scl22a3, a gene in the F$^-$N^{int} highest group, is also regulated by Air.

Differential adhesion/matrix interaction between the two cell populations was suggested in that population F$^-$N^{int} expressed high levels of tissue inhibitor of metalloproteinase 2 (Timp2), as well as the adhesion molecule integrin alpha 2b (Itga2b) and development and differentiation enhancing factor 2 (Ddef2), which acts in integrin signaling. However, this population also had the lowest mRNA level of CEA-related cell adhesion molecule 1.

Differentially expressed genes known to act in hematopoietic cell lineage include Csf1r (lowest in F$^-$N^{int}) and Itga2b (highest in F$^-$N^{int}). F$^-$N^{lo} expressed the highest levels of nephroblastoma overexpressed (Nov), a marker for the undifferentiated state necessary for effective reconstitution by human HSCs in xenograft assays (Gupta et al., 2007). Our four gene sets were relatively enriched (4.08-fold, p = 0.0162) in the GO term "regulators of cell proliferation." B cell leukemia/lymphoma 11B (Bcl11b) and the Wnt effector Tcf7 were both high in group F$^-$N^{lo}, whereas E2F transcription factor 7 (E2F7) was low in population F$^-$N^{lo} and Timp2 was high in population F$^-$N^{int}.

Of our 48 differential genes, 13 have been reported to be differentially expressed in hematopoietic stem and progenitor cells (Akashi et al., 2003; Forsberg et al., 2005; Terskikh et al., 2003; Tydell et al., 2007), confirming that they dynamically alter early in the hematopoietic lineage. For all four genes expressed highest or lowest in F$^-$N^{int} HSCs (Cnn3, Dach1, Timp2, and Csrl1), the known profile is consistent with equivalence of these HSCs and the previously studied LT-HSC/HSC population (i.e., if lowest [or highest] in F$^-$N^{int} HSCs, they are correspondingly expressed at lower [or higher] levels in LT-HSCs/HSCs than in various progenitors).

Just two of the nine genes highest or lowest in F$^-$N^{lo} (Neo1 and Socs2) fit reported expression profiles. Six with highest expression in F$^-$N^{lo} (Bclllb, Car1, Lgals, Mpo, Prtn3, and Tcf7) are either more highly expressed in ST-HSCs, multipotent progenitors (MPPs) or pro-T cells than in LT-HSCs, or more highly expressed in MPP, granulocyte-macrophage progenitors, or common myeloid progenitors than in HSCs. Likewise, Eya1 (lowest in F$^-$N^{lo}) is expressed at higher levels in HSCs than in a variety of progenitors. Thus, F$^-$N^{lo}, while functioning as LT-HSCs, may possess certain molecular properties previously ascribed to ST-HSCs or progenitors.

N-Cadherin^{int} and N-Cadherin^{lo} Stem Cells Enter the Cell Cycle at Different Rates

To assess whether F$^-$N^{int} and F$^-$N^{lo} populations differed in cell-cycle regulation, we performed prolonged labeling of cycling cells with BrdU and examined label incorporation rates, a strategy recently used to calculate the cell-cycle entry rate for CD150$^+$CD48$^-$CD41$^-$ HSCs at around 6% per day (Kiel et al., 2007a). With 1, 4, or 8 days of labeling, the percentage of BrdU$^+$ cells was consistently higher in F$^-$N^{lo} than in the F$^-$N^{int} population. After 8 days of labeling, 42% of F$^-$N^{lo} cells, but only 22% of F$^-$N^{int} cells, were BrdU$^+$ (Figures 4A and 4B). Cell-cycle entry rates, calculated by regression on the log of the proportion of unlabeled cells (Kiel et al., 2007a) (Figure 4C), revealed that ~6.7% of F$^-$N^{lo} HSCs entered the cell cycle each day, compared with only 3.2% per day for F$^-$N^{int} HSCs.

N-Cadherin and CD150 Have Distinct Expression Dynamics in HSCs

Most (67%) CD150$^+$CD48$^-$CD41$^-$ HSCs are N-cadherin^{lo} (Figure 2E), so we examined how N-cadherin and CD150

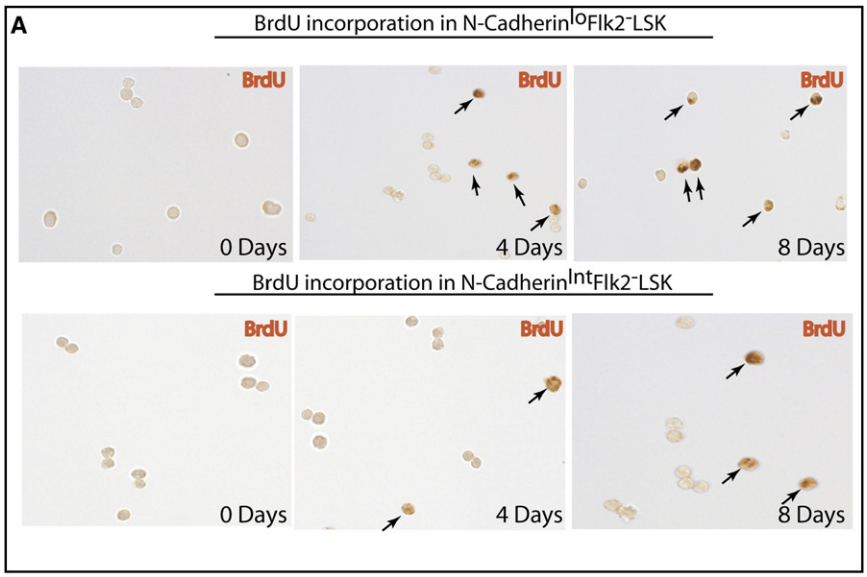

B

BrdU incorporation in N-Cadherin^{lo}Flk2^{-}LSK

	0 Days	1 Day	4 Days	8 Days
1	0	7%(26/372)	24%(28/114)	47%(100/211)
2	0	9.2%(17/173)	21%(20/95)	41%(158/395)
3	0	9%(17/183)	25%(75/321)	39%(57/147)
				Ave. 42.3%

BrdU incorporation in N-Cadherin^{Int}Flk2^{-}LSK

	0 Days	1 Day	4 Days	8 Days
1	0	5.1%(38/738)	15%(18/120)	21%(78/367)
2	0	5%(25/495)	15.1%(29/197)	20%(114/549)
3	0	6%(22/336)	16.9%(47/276)	23%(112/476)
4	0	6%(54/853)	13%(59/384)	23%(84/363)
				Ave. 21.7%

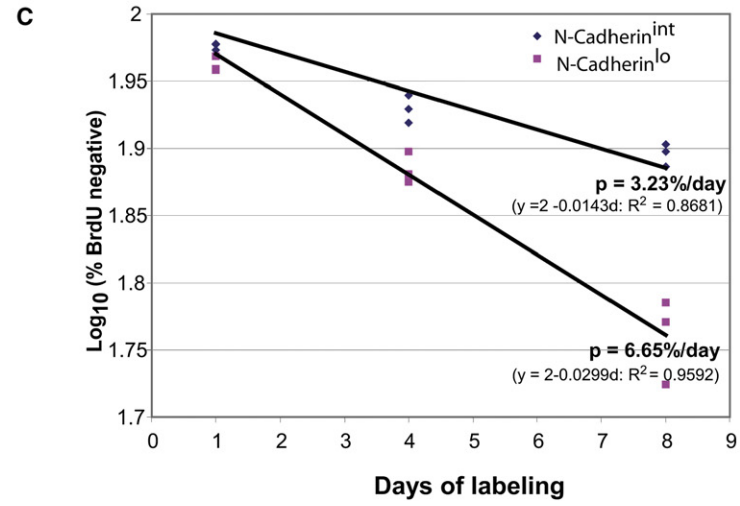

Figure 4. Comparison of Cell-Cycle Entry Rates in N-Cadherin^{lo} and N-Cadherin^{int} Flk2^{-}LSKs

(A and B) BrdU incorporation in N-cadherin^{lo} and N-cadherin^{int} Flk2^{-}LSKs after in vivo BrdU labeling for zero (negative control) 4 or 8 days. (A) Photomicrographs show representative BrdU immunostaining performed on the sorted populations indicated. Arrows indicate positive cells. (B) BrdU incorporation data expressed as percentage BrdU^{+} (number BrdU^{+}/total cells counted). Positive and negative cells were counted in a blinded study using three or four independent samples. (C) Regression of $\log_{10}$ of percent nonlabeled cells used to determine the average per day BrdU incorporation (cell-cycle entry) rate. BrdU^{+} cells may have cycled one or multiple times, complicating assessment of cell-cycle entry rate. However, if p = the proportion of cells in S phase (incorporating label) each day, then the proportion of nonlabeled cells after day d is $(1 - p)^d$. Thus, p can be calculated from the slope of log (nonlabeled cells). Regression lines assume that y = 2 at d = 0 (0% labeling at day zero). The calculated values of p are shown (as % per day). The fit of the data to each regression line is given by the R^2 value.

expression related to different states of HSCs using a population undergoing relatively synchronous activation and expansion (increase in number). A single high-dose treatment with the chemotherapeutic agent 5-fluorouracil (5FU) purges progenitors and cycling HSCs and spares primitive HSCs (Lerner and Harrison, 1990; Venezia et al., 2004) (Figure 5A). On day 3 post-5FU treatment, the LSK population was dramatically reduced (from 0.25% to 0.003%) (Figure 5B). By day 5 post-5FU, LSK numbers started to recover, indicative of HSC expansion (Figures 5B and 5C). Quantitative real-time RT-PCR on Flk2^{-}LSKs indicated mRNA levels of cyclinD1, a factor required for progression through G1, steadily increased from day 1 through 5 post-5FU (Figure 5D). N-cadherin exhibited a strong peak in mRNA expression as the LSK number reached a minimum but declined again at day 5 when expansion was underway (Figure 5E). In contrast, CD150 mRNA was low at day 3 but upregulated again in the expansion phase (Figure 5F).

To examine the coexpression pattern of N-cadherin and CD150 in individual cells, we performed single-cell RT-PCR for N-cadherin, Bmi1, CD150, and HPRT on Flk2^{-}LSKs on day 3 post-5FU. All cells analyzed were HSCs, as they expressed the self-renewal gene Bmi1 (Park et al., 2003). We also noted a largely reciprocal expression pattern between N-cadherin and CD150 (Figure 5G) on day 3 post-5FU. A low fraction of cells expressed both N-cadherin and CD150.

With flow cytometry, we were able to assay much larger numbers of cells and examine protein level expression. Under homeostatic conditions, the LSK population contained few CD150^{+} cells, and surface expression of N-cadherin and

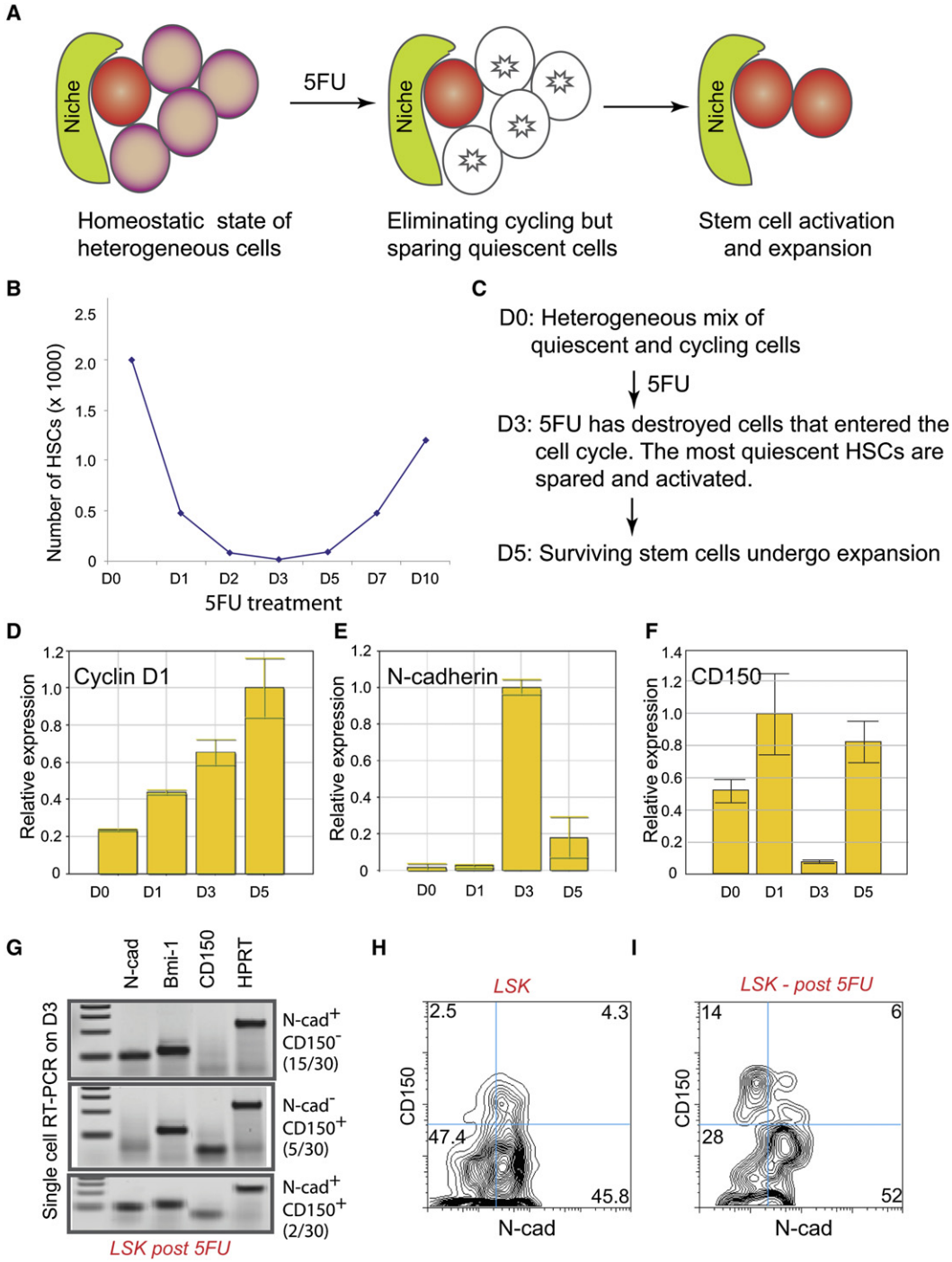

Figure 5. Examination of N-Cadherin and CD150 in HSCs Following 5FU Treatment

(A) 5FU provokes widespread changes in HSC behavior, eliminating cycling progenitors (purple) but sparing some quiescent HSCs (red). Surviving HSCs are prompted to proliferate.

(B) HSC (Flk2$^-$LSK) numbers in BM following single-dose 5FU treatment.

(C) Deduced timeline of HSC destruction, activation, and expansion.

(D–F) Effect of 5FU treatment on the mRNA expression of CyclinD1 (D), N-cadherin (E), and CD150 (F) in HSCs, assessed by quantitative real-time RT-PCR analysis of 400 Flk2$^-$LSK. Transcript level is normalized using expression of HPRT. Error bar is 1 SD.

(G) Multiplex gene expression analyses of N-cadherin, Bmi, and CD150 in single-sorted LSK cells 3 days post-5FU treatment using real-time RT-PCR with HPRT as an internal control. The fraction of the cells exhibiting each profile shown is given in parentheses.

(H and I) Examination of the change in N-cadherin and CD150 expression at the protein level in HSCs spared by 5FU treatment (I) compared to normal LSK cells (H).

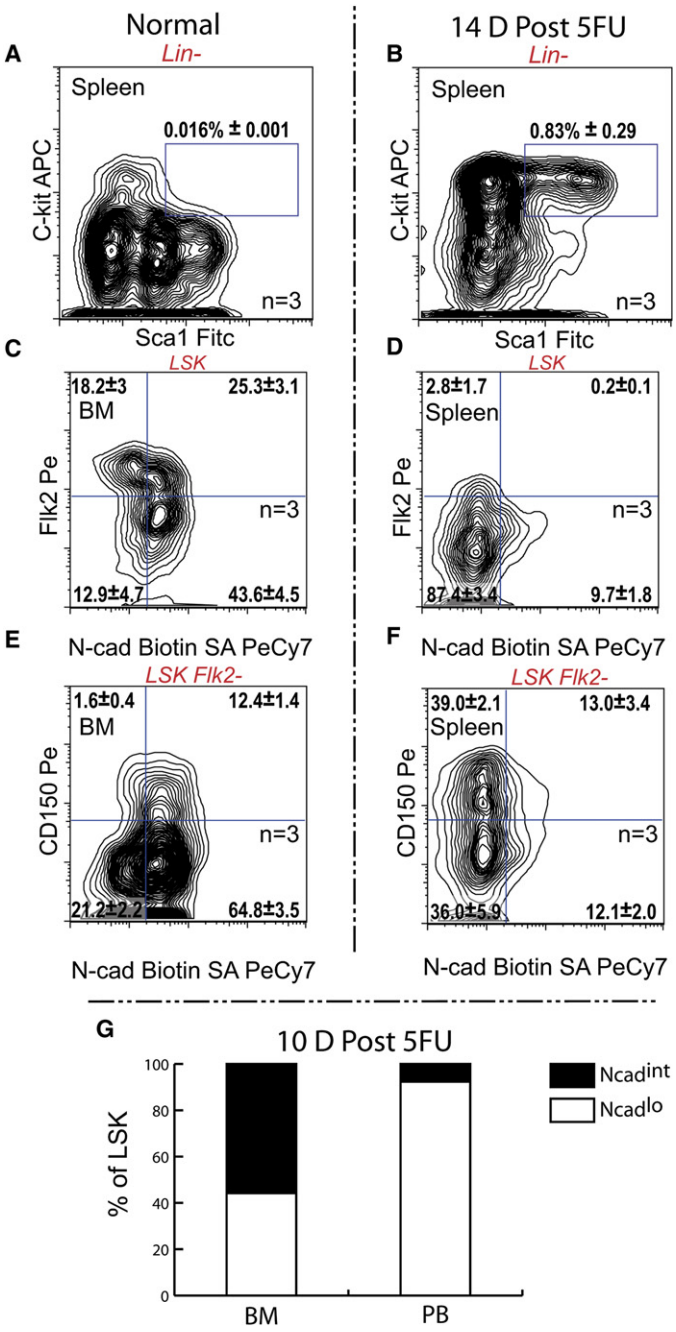

Figure 6. Examination of N-Cadherin and CD150 Expression in Mobilized HSCs

(A–F) Analysis of LSK and LT-HSCs under homeostatic conditions (A, C, and E) and 14 days post-5FU treatment (B, D, and F). (A and B) Quantification of LSKs (blue boxes) in normal spleen (A) and in spleen 14 days post-5FU. (C–F) Expression of N-cadherin and Flk2 in LSKs (C and E) or N-cadherin and CD150 in LT-HSCs (D and F) in normal BM and spleen 14 days post-5FU.

(G) Comparison of expression of N-cadherin in LSKs in BM and PB 10 days post-5FU treatment.

CD150 was not correlated (Figure 5H). Day 3 post-5FU, the N-cadherin^{lo}CD150^{-} subpopulation was depleted, and thus relatively sensitive to 5FU treatment, whereas populations with reciprocal patterns of N-cadherin and CD150 (N-cadherin^{lo}CD150^{+} and N-cadherin^{int}CD150^{-}) were relatively resistant and made up two-thirds of the LSKs (Figure 5I). Preferential destruction of the more rapidly cycling Flk2^{+} cells (including many N-cadherin^{lo} and N-cadherin^{int} cells, but few CD150^{+}) explained some, but not all, of the alteration in the N-cadherin and CD150 profile. Thus, there is differential survival of specific subpopulations of HSCs and/or coordinate and reciprocal regulation of N-cadherin and CD150 in HSCs following 5FU treatment.

Mobilized HSCs Are Predominantly N-Cadherin^{lo} Cells

Association of N-cadherin and CD150 with osteoblastic and vascular niches implies our two relatively 5FU-resistant LSK populations (N-cadherin^{int}CD150^{-} and N-cadherin^{lo}CD150^{+}) could represent HSCs residing in osteoblastic and vascular niches, respectively. Mobilized HSCs are predominantly located in the vascular niche (Kiel et al., 2005), so we examined the N-cadherin and CD150 expression profiles of HSCs mobilized to the spleen 14 days post-5FU treatment. Normally, LSKs are rarely detected in the spleen (Figure 6A); however, 2 weeks after 5FU treatment, spleen LSK number was dramatically increased, indicating mobilization of HSCs from BM (Figure 6B). In BM, just 15%–20% of Flk2^{-}LSKs were N-cadherin^{lo}, but Flk2^{-}LSKs mobilized to spleen were predominantly N-cadherin^{lo} (~87%) (Figure 6D). Spleen-mobilized HSCs were also commonly CD150^{+} cells, as indicated by the substantial increase in CD150^{+}N-cadherin^{lo} Flk2^{-}LSK cells (from 1.6% before to 39% after treatment) (compare Figures 6E and 6F). At earlier time points, mobilizing LSKs were found in PB. Ten days post 5FU, the PB LSKs were almost exclusively N-cadherin^{lo}, whereas BM LSKs were largely N-cadherin^{int} (Figure 6G). We conclude that (1) the majority of HSCs mobilized to spleen are N-cadherin^{lo}, (2) this population is also enriched with CD150^{+} cells, and (3) HSCs are N-cadherin^{lo} during mobilization and do not merely adopt this state upon arrival in a spleen vascular niche.

DISCUSSION

Low and Intermediate Levels of N-Cadherin Expression Distinguish Two HSC States

We had hoped that high N-cadherin levels might identify quiescent HSCs capable of effective reconstitution but found instead that N-cadherin^{hi} cells were mainly mature and thus incapable of reconstituting the hematopoietic system. A recent parallel study likewise showed N-cadherin^{hi} cells are not HSCs (Kiel et al., 2007b). However, analyzing a commonly studied HSC population, mouse Flk2^{-}LSKs, we found that the vast majority were confined to the N-cadherin^{int} and N-cadherin^{lo} fractions and were rarely observed as negative for or highly expressing N-cadherin.

Unexpectedly, within freshly isolated LT-HSCs, only the minority N-cadherin^{lo}Flk2^{-}LSK population (F^{-}N^{lo}) could effectively reconstitute the hematopoietic system of lethally irradiated mice, whereas the majority N-cadherin^{int} Flk2^{-}LSK population

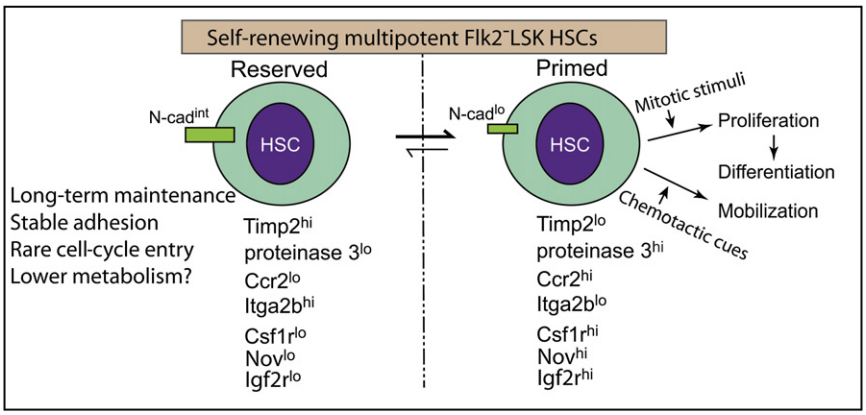

Figure 7. Model of Reserved and Primed HSCs

Properties and molecular signatures of reserved and primed states of HSCs. Reserved HSCs are adapted for long-term maintenance. Primed HSCs play a more active role in supporting hematopoiesis. Lost primed HSCs may be replaced from the larger reserved pool (bold forward arrow). Transition from primed to reserved may also occur (light reverse arrow).

(F^-N^{int}) gave only marginal levels of reconstitution. F^-N^{int} cells are, however, LT-HSCs. If briefly cultured prior to transplantation, they provided LT, multilineage reconstitution and self-renewed to generate both F^-N^{int} and F^-N^{lo} LSKs. Microarray data also firmly supported the idea that F^-N^{lo} and F^-N^{int} are two subpopulations of HSCs; only a small number of genes on the array were strongly differential between them, and both were clearly separate from the $Flk2^+$ LSK progenitors.

We also discovered F^-N^{lo} and F^-N^{int} LT-HSCs differed in mobilization efficiency and rate of cell-cycle entry. Moreover, each expressed a unique spectrum of genes that likely reflects or governs their distinct activities. These functional and molecular distinctions led us to propose a model of HSCs in which $Flk2^-$LSKs exist in either "primed" or "reserved" states that can be distinguished as N-cadherin^{lo} or N-cadherin^{int} (Figure 7).

Properties and Proposed Roles of Primed and Reserved HSCs

Our data suggest N-cadherin^{lo} HSCs (F^-N^{lo}) are specifically prepared (primed) for tasks involving reconstitution, mobilization, or response to stimuli and may have more flexible interactions with their environment. Conversely, N-cadherin^{int} HSCs (F^-N^{int}) are held back (reserved) from mobilization and may be receptive to stimuli. We propose that the normal homeostatic role of primed HSCs is active support of ongoing hematopoiesis, whereas reserved HSCs are adapted for the role of long-term maintenance.

Compared with F^-N^{int}, F^-N^{lo} HSCs express higher levels of genes involved in locomotor activity (notably Ccr2) and genes involved in signaling (Igf2r and Csf1r) and so are primed to respond more readily to migratory cues and other regulatory signals. High expression of Nov, which facilitates reconstitution ability in human HSCs (Gupta et al., 2007), further supports the argument that primed HSCs may have particular relevance in HSC transplantation. In contrast, low mRNA expression of Ccr2, Igf2r, and Csf1r implies that F^-N^{int} cells have dampened responsiveness to key growth factors and cytokines. Having a population that is insulated from migratory or other stimuli may help prevent depletion of the HSC pool.

Both homing and migration require dynamic changes in the interaction of cells with their environment such as detachment from microenvironment and transendothelial migration. One suggestive difference between F^-N^{lo} and F^-N^{int} HSCs was that F^-N^{lo} cells had lower mRNA levels of Timp2, a negative regulator of matrix metalloproteinases MMPs, and expressed more proteinase 3, an activator of MMPs (Pezzato et al., 2003) implicated in facilitating migration of hematopoietic stem/progenitor cells (Janowska-Wieczorek et al., 2000). We speculate F^-N^{lo} HSCs may possess higher MMP activity than F^-N^{int} and thus more readily remodel matrix. Conversely, reserved HSCs have higher N-cadherin protein, higher Itga2b and Timp2 mRNA, and lower proteinase 3 mRNA, suggesting a more stable relationship with their environment or niche.

Downregulation of N-cadherin itself may be required for HSC migration, which may help explain both our transplant results and our observation that mobilized HSCs are predominantly N-cadherin^{lo}. A similar concept has been reported in neural crest cells. N-cadherin expression was found to be higher either prior to or after migration when cells were anchored or were forming clusters but was downregulated when cells were actively migrating (Bronner-Fraser et al., 1992; Kasemeier-Kulesa et al., 2006).

PCA indicated F^-N^{int} HSCs are less metabolically active than F^-N^{lo} and differ in cell-cycle regulation. Indeed, the cell-cycle entry rate of F^-N^{int} HSCs (3.2% per day) is only around half that of F^-N^{lo} HSCs (6.7% per day) or SLAM code HSCs (6% per day) (Kiel et al., 2007a). Thus, reserved N-cadherin^{int} HSCs constitute a substantial pool of relatively inactive and slow-cycling LT-HSCs. Low metabolic activity and rate of proliferation could help maintain the integrity of the reserved HSC genome.

Explaining the Performance of HSC Populations in Reconstitution Assays

The difference in engraftment efficiency of fresh and cultured N-cadherin^{int} HSCs suggests these cells can be released from their reserved state but also illustrates an important consideration regarding reconstitution assays. These vital assays unfortunately impose a highly artificial challenge, which might better test a stress response rather than normal, homeostatic activity. We suggest that for fresh F^-N^{int} the very properties that fit them for their reserved role (outlined above) hamper their performance in reconstitution assays.

The modest reconstitution achieved by $CD150^+$ $Flk2^-$LSKs contrasts with the robust performance of SLAM code ($CD150^+CD41^-CD48^-$) HSCs (Kiel et al., 2005). $CD150^+$ $Flk2^-$LSKs contain reserved and primed cells in the same proportions as $Flk2^-$LSKs generally. Their reconstitution activity

thus reflects this heterogeneous but predominantly reserved makeup. We found that using CD48 and CD41 as negative markers removed not only progenitor cells but also a large portion of N-cadherin^{int} HSCs, which express higher mRNA levels of Itga2b (CD41). Thus, in the SLAM code, the negative markers effectively select primed HSCs, explaining both their robust reconstitution and the reported difficulty of detecting N-cadherin (Kiel et al., 2005, 2007b).

Transitions between Reserved and Primed HSCs

Comparing profiles of the differentially expressed genes we identified with their known expression in stem and progenitor cells (Akashi et al., 2003; Forsberg et al., 2005; Terskikh et al., 2003; Tydell et al., 2007) suggests that the primed HSC state may represent an intermediate step in a progression from reserved HSCs to the more active ST-HSC and progenitor portions of the lineage. Our culture data likewise suggest such a hierarchical relationship is possible: in culture, F^-N^{int} cells generate or become F^-N^{lo}, whereas F^-N^{lo} cultures produce a significant fraction of non-LSKs.

The greater activity/mobility of primed HSCs places them at risk for depletion, when lost primed HSCs may be replaced by cells from the reserved pool. Equally, under some situations, primed HSCs may revert to a reserved state (Figure 7). For example, upon transplantation or after homing to BM, some primed cells may occupy vacant niches that impose a reserved state. We found that transplant of cultured reserved cells can generate a normal pattern of both primed and reserved HSCs in recipient mice. We also observed dynamic changes in N-cadherin expression following 5FU treatment with primed HSCs ultimately mobilized to PB and spleen. A recent report suggests that reactive oxygen species (ROS) generated by 5FU suppresses N-cadherin expression in HSCs, causing them to detach from the osteoblastic niche. Thus, ROS may trigger a shift in HSC state (Hosokawa et al., 2007).

Osteoblastic and Vascular Niches May Differentially Regulate HSC States

Finding that HSCs can be divided into primed and reserved pools raises the question of whether these pools reside in physically separate locations. Previous studies suggest that N-cadherin may form an adherent junction between HSCs and the osteoblastic niche maintaining HSCs as quiescent (Arai et al., 2004; Zhang et al., 2003). We therefore suggest that reserved (N-cadherin^{int}) HSCs favor the osteoblastic niche. SLAM code HSCs are known to occupy a vascular niche (Kiel et al., 2005). The observations that (1) SLAM code cells are mainly N-cadherin^{lo} HSCs (Figure 2E), (2) homing and mobilized HSCs are enriched with N-cadherin^{lo} and Slamf1$^+$ cells (Figures 6D, 6F, and 6G), and (3) N-cadherin^{lo} HSCs and SLAM code HSCs have similar cell-cycle entry rates (Kiel et al., 2007a) (Figure 4C) suggest that primed HSCs may tend to occupy a vascular niche. A recent report that HSCs residing in the osteoblastic niche have higher N-cadherin levels than those in the vascular niche supports this concept (Jang and Sharkis, 2007). However, further studies are needed to rigorously establish any relationship between reserved and primed cells and osteoblastic or vascular niches.

Disrupting one niche type highlights the role of others. If the osteoblastic niche contains mostly reserved cells, loss or modulation of this niche might have little immediate impact on tissue regeneration. The level of disruption/reduction of niches may determine phenotype. Biglycan deficiency, which leads to a reduction in osteoblast number and trabecular bone, is reported not to alter HSC number (Kiel et al., 2007b), yet numerous other studies have demonstrated the importance of osteoblasts as well as osteoclasts, which function in bone remodeling, in controlling the number and long-term maintenance of HSCs (reviewed in Scadden, 2006; Yin and Li, 2006; Kollet et al., 2006; Walkley et al., 2007a). RARγ-deficient and Rb mutant mice with severe reduction in trabecular bone or osteoblasts result in HSC mobilization from BM to spleen, short-term expansion of HSCs and development of myeloid proliferative disorder (Walkley et al., 2007a, 2007b). Such changes, consistent with the proposed functions of the vascular niche in supporting proliferation and myeloid differentiation (Kopp et al., 2005), may also be seen as an enforced primed phenotype. Irrespective of where they are ultimately located, our demonstration that HSCs are in distinct reserved and primed states provides a useful framework for studying and using stem cells.

EXPERIMENTAL PROCEDURES

Animals

All mice used in this study were housed in the animal facility at Stowers Institute for Medical Research (SIMR) and handled according to Institute and National Institutes of Health (NIH) guidelines. All procedures were approved by the Institutional Animal Care and Use Committee of SIMR.

Antibody Generation

The anti-N-cadherin mAb was generated from MNCD2 hybridoma cells (obtained from the Hybridoma Bank) injected into nude mice. Ascites fluid was harvested from which antibodies were purified. These were conjugated with biotin or phycoerythrin (by Rockland Immunochemicals, Gilbertsville, PA) or were left unconjugated.

Flow Cytometry Analysis of Hematopoietic Cells

Hematopoietic cells were harvested from spleen, PB, and BM in the femurs and tibias. Red blood cells were lysed using a 0.30M ammonium chloride solution. For cell surface phenotyping, a lineage cocktail (Lin) was used composed of mAbs recognizing the following markers: CD3, CD4, CD8, CD11b (Mac1), CD45R (B220), Gr1, IgM, and Ter119 (eBioscience, San Diego, CA). Monoclonal antibodies against Sca1, cKit, Flk2, CD41, CD48 (eBioscience), CD150 (BioLegend, San Diego, CA), and N-cadherin (see above) were also used. For isolation of HSCs, Dynal sheep-anti-Rat magnetic beads (Invitrogen, Carlsbad, CA) were used with the Lin cocktail to remove the majority of Lin$^+$ cells. The remaining Lin$^-$-enriched cells were incubated with appropriate antibodies for further purification using flow cytometry. Cell sorting and analysis were performed using the MoFlo (Dako, Ft. Collins, CO) and/or the CyAn ADP (Dako, Ft. Collins, CO).

Competitive Reconstitution Assay

Ten, twenty-five, or one hundred LSK cells from B6 (CD45.2) mouse BM, subdivided by expression of combinations of Flk2, N-cadherin, and/or CD150, were transplanted with 2×10^5 Ptprc (CD45.1) BM cells into lethally irradiated Ptprc mice via tail vein injection. Posttransplantation PB samples were taken from recipient mice and analyzed at 1, 2, 3, 4, or 6 months. The cells were incubated with mAbs against CD45.1, CD45.2, CD11b, Gr1, CD3, and CD45R (eBioscience). Successful engraftment was defined as the presence of a distinct CD45.2$^+$CD45.1$^-$ population above a background set by parallel analysis of animals transplanted with only rescue BM.

RNA Amplification for Microarray Analysis

Methods for RNA extraction, amplification, and microarray analysis were previously described (Akashi et al., 2003). The result of hybridization of the derived cRNA to MouseGenome430_2 arrays was scanned with a GeneChip Scanner 3000 7G using GeneChip Fluidics Station 450 and GeneChip Operating Software (GCOS 1.4).

5-Fluorouracil Treatment

Mice were injected once via tail vein with 5FU at 150–300 μg/g body weight. BM and/or spleen tissue was harvested either 1, 3, 5, 7, 10, or 14 days post 5FU treatment.

Quantitative Real-Time RT-PCR

Twelve hundred (1200) N-cadherin^{+}, Lin^{-}N-cadherin^{-}, Lin^{-}N-cadherin^{lo}, Lin^{-}N-cadherin^{int}, Flk2^{-}LSK, N-cad^{lo}Flk2^{-}LSK, and N-cad^{int}Flk2^{-}LSK BM cells were directly sorted into 800 μl Trizol (Ambion, Austin TX). RNA was extracted and treated for 20 min at 37°C with 2 μl RNase-free DNase-1 (2 U/μl; Ambion) in the presence of 2 μl RNase inhibitor (10 U/μl; Invitrogen). For each real-time RT-PCR reaction, RNA from each type of sorted cell was divided to three reactions equivalent to 400 cells.

N-cadherin primers (F2074, 5′AGCGCAGTCTTACCGAAGG, and R2075, 5′TCGCTGCTTTCATACTGAACTTT) were designed to generate 101 bp amplicon spanning the exon2/3 boundary. Real-time RT-PCR reactions were performed using an iCycler (Bio-Rad iQ5) according to the manufacturer's instructions. Amplification of hypoxanthine phosphoribosyl transferase (HPRT) was used to normalize for sample RNA content. Specificity of products was confirmed by melting curve analysis, assessing band size in 2% agarose gels, and DNA sequencing.

Multiplex Gene Analysis in Single-Cell Using RT-PCR

Multiplex single-cell RT-PCR analysis was performed as described previously (Akashi et al., 2003) with primers specific for Bmi-1, N-cadherin (F2100, 5′TGCAAGACTGGATTTCCTGA, and R2101, 5′CTCTGCAGTGAGAGGG AAGC), Slamf1 (CD150), and HPRT. First-round PCR was performed in the same plate as the RT by adding premixed PCR buffer containing all gene-specific forward and reverse primers. Second-round PCR with fully nested primers (F2074 and R2075 for N-cadherin) was performed separately for each gene on 4% aliquots of first-round product.

ACCESSION NUMBERS

The microarray data are available at ArrayExpress (http://www.ebi.ac.uk/arrayexpress/) under accession number E-TABM-404.

SUPPLEMENTAL DATA

Supplemental Data include three figures, three tables, Supplemental Experimental Procedures, and Supplemental References and can be found with this article online at http://www.cellstemcell.com/cgi/content/full/2/4/367/DC1/.

ACKNOWLEDGMENTS

We thank Drs. Leanne M. Wiedemann, Robb Krumlauf, William Neaves, and Toshio Suda for scientific discussion; Dr. Dongxiao Zhu for statistical help; and Donna di Natale and Karen Tannen for manuscript proofreading and editing. We appreciate technical support from Teri Johnson, Heather Marshall, and David Scoville. The Stowers Institute for Medical Research funded this work.

Received: August 24, 2007
Revised: December 10, 2007
Accepted: January 23, 2008
Published: April 9, 2008

REFERENCES

Akashi, K., He, X., Chen, J., Iwasaki, H., Niu, C., Steenhard, B., Zhang, J., Haug, J., and Li, L. (2003). Transcriptional accessibility for genes of multiple tissues and hematopoietic lineages is hierarchically controlled during early hematopoiesis. Blood *101*, 383–389.

Arai, F., Hirao, A., Ohmura, M., Sato, H., Matsuoka, S., Takubo, K., Ito, K., Koh, G.Y., and Suda, T. (2004). Tie2/angiopoietin-1 signaling regulates hematopoietic stem cell quiescence in the bone marrow niche. Cell *118*, 149–161.

Balazs, A.B., Fabian, A.J., Esmon, C.T., and Mulligan, R.C. (2006). Endothelial protein C receptor (CD201) explicitly identifies hematopoietic stem cells in murine bone marrow. Blood *107*, 2317–2321.

Bronner-Fraser, M., Wolf, J.J., and Murray, B.A. (1992). Effects of antibodies against N-cadherin and N-CAM on the cranial neural crest and neural tube. Dev. Biol. *153*, 291–301.

Calvi, L.M., Adams, G.B., Weibrecht, K.W., Weber, J.M., Olson, D.P., Knight, M.C., Martin, R.P., Schipani, E., Divieti, P., Bringhurst, F.R., et al. (2003). Osteoblastic cells regulate the haematopoietic stem cell niche. Nature *425*, 841–846.

Christensen, J.L., and Weissman, I.L. (2001). Flk-2 is a marker in hematopoietic stem cell differentiation: a simple method to isolate long-term stem cells. Proc. Natl. Acad. Sci. USA *98*, 14541–14546.

Fleming, W.H., Alpern, E.J., Uchida, N., Ikuta, K., Spangrude, G.J., and Weissman, I.L. (1993). Functional heterogeneity is associated with the cell cycle status of murine hematopoietic stem cells. J. Cell Biol. *122*, 897–902.

Forsberg, E.C., Prohaska, S.S., Katzman, S., Heffner, G.C., Stuart, J.M., and Weissman, I.L. (2005). Differential expression of novel potential regulators in hematopoietic stem cells. PLoS Genet. *1*, e28. 10.1371/journal.pgen.0010028.

Gupta, R., Hong, D., Iborra, F., Sarno, S., and Enver, T. (2007). NOV (CCN3) functions as a regulator of human hematopoietic stem or progenitor cells. Science *316*, 590–593.

Hosokawa, K., Arai, F., Yoshihara, H., Nakamura, Y., Gomei, Y., Iwasaki, H., Miyamoto, K., Shima, H., Ito, K., and Suda, T. (2007). Function of oxidative stress in the regulation of hematopoietic stem cell-niche interaction. Biochem. Biophys. Res. Commun. *363*, 578–583.

Jang, Y.-Y., and Sharkis, S.J. (2007). A low level of reactive oxygen species selects for primitive hematopoietic stem cells that may reside in the low-oxygenic niche. Blood *110*, 3056–3063.

Janowska-Wieczorek, A., Marquez, L.A., Dobrowsky, A., Ratajczak, M.Z., and Cabuhat, M.L. (2000). Differential MMP and TIMP production by human marrow and peripheral blood CD34(+) cells in response to chemokines. Exp. Hematol. *28*, 1274–1285.

Kasemeier-Kulesa, J.C., Bradley, R., Pasquale, E.B., Lefcort, F., and Kulesa, P.M. (2006). Eph/ephrins and N-cadherin coordinate to control the pattern of sympathetic ganglia. Development *133*, 4839–4847.

Kiel, M.J., Yilmaz, O.H., Iwashita, T., Terhorst, C., and Morrison, S.J. (2005). SLAM family receptors distinguish hematopoietic stem and progenitor cells and reveal endothelial niches for stem cells. Cell *121*, 1109–1121.

Kiel, M.J., He, S., Ashkenazi, R., Gentry, S.N., Teta, M., Kushner, J.A., Jackson, T.L., and Morrison, S.J. (2007a). Haematopoietic stem cells do not asymmetrically segregate chromosomes or retain BrdU. Nature *449*, 238–242.

Kiel, M.J., Radice, G.L., and Morrison, S.J. (2007b). Lack of evidence that hematopoietic stem cells depend on N-cadherin-mediated adhesion to osteoblasts for their maintenance. Cell Stem Cell *1*, 204–217.

Kollet, O., Dar, A., Shivtiel, S., Kalinkovich, A., Lapid, K., Sztainberg, Y., Tesio, M., Samstein, R.M., Goichberg, P., Spiegel, A., et al. (2006). Osteoclasts degrade endosteal components and promote mobilization of hematopoietic progenitor cells. Nat. Med. *12*, 657–664.

Kopp, H.G., Avecilla, S.T., Hooper, A.T., and Rafii, S. (2005). The bone marrow vascular niche: home of HSC differentiation and mobilization. Physiology (Bethesda) *20*, 349–356.

Lerner, C., and Harrison, D.E. (1990). 5-Fluorouracil spares hemopoietic stem cells responsible for long-term repopulation. Exp. Hematol. *18*, 114–118.

Luo, Y., Kostetskii, I., and Radice, G.L. (2005). N-cadherin is not essential for limb mesenchymal chondrogenesis. Dev. Dyn. *232*, 336–344.

Moser, B., Wolf, M., Walz, A., and Loetscher, P. (2004). Chemokines: multiple levels of leukocyte migration control. Trends Immunol. *25*, 75–84.

Muguruma, Y., Yahata, T., Miyatake, H., Sato, T., Uno, T., Itoh, J., Kato, S., Ito, M., Hotta, T., and Ando, K. (2006). Reconstitution of the functional human hematopoietic microenvironment derived from human mesenchymal stem cells in the murine bone marrow compartment. Blood *107*, 1878–1887.

Park, I.K., Qian, D., Kiel, M., Becker, M.W., Pihalja, M., Weissman, I.L., Morrison, S.J., and Clarke, M.F. (2003). Bmi-1 is required for maintenance of adult self-renewing haematopoietic stem cells. Nature *423*, 302–305.

Pezzato, E., Dona, M., Sartor, L., Dell'Aica, I., Benelli, R., Albini, A., and Garbisa, S. (2003). Proteinase-3 directly activates MMP-2 and degrades gelatin and Matrigel; differential inhibition by (−)epigallocatechin-3-gallate. J. Leukoc. Biol. *74*, 88–94.

Raychaudhuri, S., Stuart, J.M., and Altman, R.B. (2000). Principal components analysis to summarize microarray experiments: application to sporulation time series. Pac. Symp. Biocomput., 455–466.

Roederer, M. (2001). Spectral compensation for flow cytometry: visualization artifacts, limitations, and caveats. Cytometry *45*, 194–205.

Scadden, D.T. (2006). The stem-cell niche as an entity of action. Nature *441*, 1075–1079.

Schofield, R. (1978). The relationship between the spleen colony-forming cell and the haemopoietic stem cell. Blood Cells *4*, 7–25.

Sleutels, F., Zwart, R., and Barlow, D.P. (2002). The non-coding Air RNA is required for silencing autosomal imprinted genes. Nature *415*, 810–813.

Song, X., and Xie, T. (2002). DE-cadherin-mediated cell adhesion is essential for maintaining somatic stem cells in the Drosophila ovary. Proc. Natl. Acad. Sci. USA *99*, 14813–14818.

Terskikh, A.V., Miyamoto, T., Chang, C., Diatchenko, L., and Weissman, I.L. (2003). Gene expression analysis of purified hematopoietic stem cells and committed progenitors. Blood *102*, 94–101.

Tucker, K.L., Meyer, M., and Barde, Y.-A. (2001). Neurotrophins are required for nerve growth during development. Nat. Neurosci. *4*, 29–37.

Tydell, C.C., David-Fung, E.-S., Moore, J.E., Rowen, L., Taghon, T., and Rothenberg, E.V. (2007). Molecular dissection of prethymic progenitor entry into the T lymphocyte developmental pathway. J. Immunol. *179*, 421–438.

Venezia, T.A., Merchant, A.A., Ramos, C.A., Whitehouse, N.L., Young, A.S., Shaw, C.A., and Goodell, M.A. (2004). Molecular signatures of proliferation and quiescence in hematopoietic stem cells. PLoS Biol. *2*, e301. 10.1371/journal.pbio.0020301.

Walkley, C.R., Olsen, G.H., Dworkin, S., Fabb, S.A., Swann, J., McArthur, G.A., Westmoreland, S.V., Chambon, P., Scadden, D.T., and Purton, L.E. (2007a). A microenvironment-induced myeloproliferative syndrome caused by retinoic acid receptor gamma deficiency. Cell *129*, 1097–1110.

Walkley, C.R., Shea, J.M., Sims, N.A., Purton, L.E., and Orkin, S.H. (2007b). Rb regulates interactions between hematopoietic stem cells and their bone marrow microenvironment. Cell *129*, 1081–1095.

Wilson, A., Murphy, M.J., Oskarsson, T., Kaloulis, K., Bettess, M.D., Oser, G.M., Pasche, A.C., Knabenhans, C., Macdonald, H.R., and Trumpp, A. (2004). c-Myc controls the balance between hematopoietic stem cell self-renewal and differentiation. Genes Dev. *18*, 2747–2763.

Yin, T., and Li, L. (2006). The stem cell niches in bone. J. Clin. Invest. *116*, 1195–1201.

Zhang, J., Niu, C., Ye, L., Huang, H., He, X., Tong, W.G., Ross, J., Haug, J., Johnson, T., Feng, J.Q., et al. (2003). Identification of the haematopoietic stem cell niche and control of the niche size. Nature *425*, 836–841.

Zhang, C.C., Kaba, M., Ge, G., Xie, K., Tong, W., Hug, C., and Lodish, H.F. (2006). Angiopoietin-like proteins stimulate ex vivo expansion of hematopoietic stem cells. Nat. Med. *12*, 240–245.